Accepted Manuscript

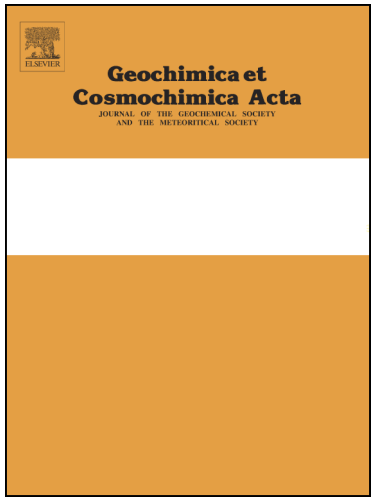

Multi-specimen and multi-site calibration of Aleutian coralline algal Mg/Ca to sea surface temperature

B. Williams, J. Halfar, K.L. DeLong, S. Hetzinger, R.S. Steneck, D.E. Jacob

PII: S0016-7037(14)00228-2
DOI: http://dx.doi.org/10.1016/j.gca.2014.04.006
Reference: GCA 8756

To appear in: *Geochimica et Cosmochimica Acta*

Received Date: 21 July 2013
Accepted Date: 3 April 2014

Please cite this article as: Williams, B., Halfar, J., DeLong, K.L., Hetzinger, S., Steneck, R.S., Jacob, D.E., Multi-specimen and multi-site calibration of Aleutian coralline algal Mg/Ca to sea surface temperature, *Geochimica et Cosmochimica Acta* (2014), doi: http://dx.doi.org/10.1016/j.gca.2014.04.006

Multi-specimen and multi-site calibration of Aleutian coralline algal Mg/Ca to sea surface temperature

B. Williams[1,2], J. Halfar[2], K.L. DeLong[3], S. Hetzinger[4], R.S. Steneck[5], and D.E. Jacob[6]

1. W.M. Keck Science Department, Claremont McKenna College-Pitzer College-Scripps College, Claremont, CA, USA

2. Department of Chemical and Physical Sciences, University of Toronto, Mississauga, ON, Canada

3. Department of Geography and Anthropology, Louisiana State University, Baton Rouge, LA, USA

4. GEOMAR Helmholtz Centre for Ocean Research Kiel, Wischhofstr. 1-3, 24148 Kiel, Germany

5. Darling Marine Center, University of Maine, Walpole, Maine, USA

6. Department of Earth and Planetary Sciences, Macquarie University, North Ryde, NSW 2109, Sydney, Australia

ABSTRACT

Higher latitude oceanic and climatic reconstructions are needed to distinguish natural climate variability from anthropogenic warming in regions projected to experience significant increases in temperature during this century. *Clathromorphum nereostratum* is a long-lived coralline alga abundant along the Aleutian archipelago that records seasonal to centennial fluctuations in seawater temperatures in its high-Mg calcite skeleton. Thus, *C. nereostratum* is an important proxy archive to reconstruct past seawater temperature variability in this data-poor subarctic region. Here, we measured magnesium to calcium ratios (Mg/Ca) by laser ablation-inductively coupled plasma-mass spectrometry (LA-ICP-MS) along the growth axis in six live-collected specimens from three islands in the Aleutian archipelago to assess Mg/Ca reproducibility and to calibrate algal Mg/Ca against modern gridded sea surface temperature (SST) data products. The master Mg/Ca-SST transfer function, determined by averaging the algal Mg/Ca-SST from each island (n=6), resulted in a reconstruction error of ±0.45°C, a 31 to 46% reduction in error compared to the reconstruction error for a single alga. The master algal-SST record interpolated to monthly and annual resolution significantly varied with gridded SST data products (r^2=0.98, p<0.0001, n=517 and r^2=.27, p<0.0003, n=44, respectively) for the period from 1960 to 2003. Therefore, coralline algal Mg/Ca-derived SST reconstructions record absolute changes in past SST variability in the Aleutian archipelago. The transfer functions developed here can be applied to Mg/Ca records generated from long-lived specimens of *C. nereostratum* to reconstruct northern North Pacific and Bering Sea SST variability for the past several hundred years.

1. INTRODUCTION

Higher latitude regions are projected to experience the largest increase in temperatures as a result of rising greenhouse gases during this century (Meehl et al., 2006; Solomon et al., 2007). These regions significantly impact global climate, primarily through the influence of sea ice albedo-climate feedback

mechanism (IPCC, 2013; Lamb, 1965) and atmospheric teleconnections (Gregory et al., 2013). Yet, deficiencies in instrumental temperature data sets make detection of high latitude change difficult (Lamb, 1977), as well as limiting our understanding of high latitude ocean-climate processes (Bourassa et al., 2013). Gridded and interpolated sea surface temperature (SST) data products derived from ship of opportunity observations are globally available yet the number of observations for any single gridded area are reduced prior to 1950 (Deser et al., 2010). Therefore, high-resolution reconstructions from proxy archives are needed to extend the available data sets back more than several decades to address questions on climate variability in the early 20th century and preceding anthropogenic warming (Bourassa et al., 2013). There are few such archives of ocean temperature for the high latitude oceans, thus limiting our understanding of past oceanic change on monthly-to-centennial time scales.

The high-resolution climate archives available at the higher latitude oceanic environments such as deep-sea corals and bivalves are limited in their distribution, contain biological-induced variability in their geochemically-derived reconstructions (Torres et al., 2011), or are located deeper in the water column and do not provide information about surface water variability. However, geochemical and sclerochronological records extracted from long-lived encrusting coralline alga *Clathromorphum* sp. are now providing significant records of higher latitude climate and ocean variability (Chan et al., 2011; Halfar et al., 2013; Halfar et al., 2007; Halfar et al., 2011b; Hetzinger et al., 2012; Williams et al., 2011). *Clathromorphum* sp. is very abundant in near-surface rocky seafloor environments throughout the mid-to-high latitudes in the northern hemisphere and can grow for hundreds of years with specimens dating back nearly a millennium (Adey et al., Accepted; Halfar et al., 2007). This alga forms clear annual growth increments in its high-Mg calcite skeleton in response to winter decreases in temperature and insolation, and onset of reproduction such that large, poorly calcified cells in the spring overlay short, heavily calcified cells formed during the previous winter (Figure 1a) (Adey, 1965; Adey et al., Accepted; Moberly, 1968). The $\delta^{18}O$ and Mg/Ca variations along the growth axis in the skeletons of *Clathromorphum* sp. vary in response to variations in SST (Halfar et al., 2008; Halfar et al., 2007; Hetzinger et al., 2009; Moberly, 1968). Despite the high biological variability in growth rates among *Clathromorphum* sp. specimens (Halfar et al., 2011a; Halfar et al., 2011b), the geochemical variability within a specimen or among specimens has not been fully assessed because previous studies generally rely on few specimens due to the analytical expense and time constraints of analyzing replicate transects in multiple specimens (Halfar et al., 2008; Halfar et al., 2007; Hetzinger et al., 2009; Hetzinger et al., 2012; Hetzinger et al., 2013). Yet, it is important to understand the intra- and inter-specimen geochemical variability so that environmentally-driven variability in the algal skeleton can be separated from biological variability and confidence intervals can be established for interpreting the records generated

from geochemical measurements (de Villiers et al., 1995; DeLong et al., 2007; DeLong et al., 2013). Therefore, robust assessments of skeletal Mg/Ca with SST records are needed prior to confidently extending Mg/Ca-derived SST reconstructions into the past.

In this study, we measure replicated transects of Mg/Ca in six specimens of *Clathromorphum nereostratum* from three islands in the Aleutian archipelago in the North Pacific and Bering Sea. We use these transects to assess geochemically-, biologically-, and environmentally-driven variability in skeletal Mg/Ca. We then determine a master transfer function for algal Mg/Ca to SST. The algal Mg/Ca calibration and uncertainty assessment developed here is a critical step to using *C. nereostratum* to reconstruct past absolute temperature variability for multi-centennial timescales in the ecologically and economically significant northern North Pacific Ocean and Bering Sea regions.

2. METHODS

2.1. Study Area and climatology

This study examines six *C. nereostratum* specimens collected from Attu, Amchitka, and Akun Islands spanning 20° of longitude in the Aleutian archipelago (Figure 2). The Aleutian archipelago is a chain of volcanic islands extending westward from the Gulf of Alaska toward the Kamchatka Peninsula, separating the North Pacific Ocean to the south from the Bering Sea to the north. The Alaskan Stream, originating in the Gulf of Alaska, brings warmer water westward along the south side of the archipelago before turning into the Bering Sea through the Aleutian Islands passages where it is the dominant source of relatively warm, fresh, and nutrient-rich water (Reed and Stabeno, 1994). Previous temperature reconstructions in this region using single coralline alga specimens indicate the central Aleutian archipelago is sensitive to climate patterns that influence the North Pacific Ocean and the Bering Sea, such as the Pacific Decadal Oscillation, and teleconnections into the region from the northern Atlantic Ocean including the North Atlantic Oscillation (Halfar et al., 2007; Hetzinger et al., 2009; Hetzinger et al., 2012).

Globally complete and interpolated gridded monthly SST data products (Kaplan et al., 1998; Rayner et al., 2003; Reynolds et al., 2002; Reynolds and Smith, 1994) are reconstructions using historical nautical records archived in the International Comprehensive Ocean-Atmosphere Data Set (ICOADS) database (Worley et al., 2005) for the interval before satellite-based observations (before 1981). The authors of these monthly SST data products use numerical methods to complete grid cells with missing observations by interpolating from grids cells with observations, generally from coastal regions and shipping lanes. Because local SST observations are not available at locations where the algal specimens were collected in

this study, we extracted SST time series for 1º grid areas that include our study sites from two SST data products: the NOAA Optimum Interpolation Sea Surface Temperature (OISST; 1981–2003) (Reynolds et al., 2002) and the Hadley Centre Interpolated Sea Surface Temperature (HadlSST; 1960–2003) (Rayner et al., 2003). The OISST data product includes satellite-derived SST estimates thus providing complete spatial and temporal coverage (Reynolds et al., 2002). The HadISST data product also includes satellite SST estimates from 1981 to present; however, before 1981 interpolated SST estimates are used when no observations are available (Rayner et al., 2003). The number of ICOADS SST observations for the 2° grid boxes that contain our study sites steeply decrease prior to the early 1960s (see Figure 3 for observations for the larger grid 50-56°N by 172°E-162°W) (Black et al., 2009; Deser et al., 2010; Hetzinger et al., 2012). Thus, SST from these data products pre-1960s are less likely to capture the full range of seasonal variability and only SSTs post-1960 were used.

Maximum SST occurs during August or September and minimum SST occurs during February, March, or April in the Aleutian archipelago (Figure 4). Monthly SST extremes range between 2.3°C to 11.1°C surrounding Attu Island, 2.9°C to 10.4°C surrounding Amchitka Island, and 2.5°C to 11.5°C surrounding Akun Island for the period from 1982 to 2003 (determined from OISST; Figure 4b). The average monthly maximum SST at Amchitka Island (9.2°C ±0.7, 1σ) is significantly different from Attu and Akun Islands (p=0.003 and p<0.0001, respectively, n=22) whereas Attu Island (9.8°C ±0.6, 1σ) is not significantly different from Akun Island (10.1°C ±0.6, 1σ; p=0.1, n=22) (Figure 4b). The average monthly minimum SST is similar for all three islands (Figure 4b). Average annual temperatures differ by 1.1°C for Attu and Amchitka Islands and by 1.4°C for Akun Island and the other islands for the period from 1982 to 2003 (Figure 4c). We find similar variability in SST among the islands for the HadISST data product, although minimum monthly values were on average 0.2°C cooler and the maximum monthly values were on average 0.3°C warmer than the OISST dataset when compared for the common period of 1982 to 2003 (Figure 4).

2.2. Specimen collection

Divers using SCUBA during field expeditions in August 2004 and June 2008 collected six living plants of *C. nereostratum* from 10 m water depth. Two specimens were collected from each island (Table 1). Specimen sizes ranged from several centimeters to tens of centimeters (Figure 1a).

Specimens were air-dried and then sectioned perpendicular to the direction of maximum growth using a large rock saw at the University of Toronto. Thick sections were polished to three microns and high-resolution images were generated using an Olympus reflected light microscope (VS-BX) attached to an

automated sampling stage/imaging system equipped with the software geo.TS (Olympus Soft Imaging Systems). The resulting images were stitched together to form a single very high-resolution photomosaic of each section (Figure 1b). The skeletal structure of each specimen was closely examined in the high-resolution digital images to ensure that no growth discontinuities were present along transects selected for geochemical analysis. The geo.TS software was used to select two approximately parallel digital paths along the axis of maximum growth on the photomosaic for each specimen avoiding the conceptacles. Conceptacles are the spheroidal cavities used for reproduction formed in part by the dissolution of previously calcified skeleton (Figure 1b). Coordinates of the two digital pathways along with two reference points for each specimen were transferred to the automated stage of the laser ablation-inductively coupled plasma-mass spectrometry (LA-ICP-MS) system used to measure Mg/Ca ratios.

2.3. Specimen analysis

Microprobe Mg/Ca values for specimen 11-4 from Attu Island were previously reported by Hetzinger et al. (2009) and the LA-ICP-MS Mg/Ca values for specimens 8-24 and 8-27 from Akun Island were previously reported by Chan et al. (2011). Here, isotopes of ^{24}Mg and ^{43}Ca were measured following the protocols outlined in Hetzinger et al. (2011) using an Agilent 7500ce quadrupole ICP-MS coupled to a New Wave Research UP-213 laser ablation system (213 nm wavelength, Nd:YAG Laser) with helium as carrier gas located at the Department of Geosciences, Johannes Gutenberg-Universität, Mainz, Germany. Continuous transects were ablated 65 µm in width with a scan speed of 10 µm s^{-1} and a laser energy density of 6 J cm^{-2}. Each transect was pre-ablated with the same energy density but higher scan speed of 100 µm s^{-1}. For details on instrumental parameters, sensitivity, typical analytical error and reproducibility, see Jacob (2006).

At least 4500 LA-ICP-MS data points were measured for each transect (Figure 5). This laser system is equipped with a large format cell (15.5 cm x 15.5 cm) permitting specimens to be measured in their entirety at one time. NISTSRM610 glass (US National Institute of Standard and Technology Standard Reference Material) was used as the external standard. The standard deviation of repeated analyses of the NISTSR610 every 30 minutes was always within 10%, indicating that instrumental drift with time was insignificant. The relative standard deviation (RSD) for repeated analysis of NISTSRM610 (single spots) was less than 2% for $^{24}Mg/^{43}Ca$. Analytical error was based on uncertainty of the reported Mg and Ca values in the NISTSR610 standard (Mg/Ca = 0.0055 g/g (Pearce et al., 1997) with a measured uncertainty of 0.00033 g/g). This uncertainty was propagated through the calculations relating the relative Mg/Ca values measured in the sample to the absolute concentrations in the sample. Using this method, average

analytical uncertainty for measurements with higher Mg/Ca values was 0.011 mol/mol (1σ) and for measurements with lower Mg/Ca values was 0.006 mol/mol (1σ) (Figure 5).

2.3.1 Non-matrix matched calibration and choice of laser wavelength

Using the NIST 610 reference glass for standardization, although this does not match the carbonate matrix of the samples, bears critical advantages over the use of a carbonate reference material. To date only one suitable matrix-matched reference material exists (USGS MACS 3) whose trace element concentrations are known to a much lower accuracy than the well-studied NIST SRM 610 glass (GeoReM database; Jochum et al., 2005). Since the extended uncertainty of analysis (Jochum et al., 2012) is a function of the analytical uncertainty on the values in the reference material in addition to crater aspect ratios and matrix, the advantages of using NIST SRM glasses outweigh the disadvantages of an unmatched matrix. The extended uncertainty on Mg is in fact twice as high (16%, Jochum et al. (2012) their Table 1) for MACS3 than that for NIST 610 (6%).

It is generally recommendable to use the 193 nm wavelength for trace element measurements in carbonate materials to minimize fractionation effects (Czas et al., 2012; Hathorne et al., 2007; Jochum et al., 2012). However, these element fractionation effects are largest for siderophile elements, while lithophile elements like Mg are less or not at all affected (Czas et al., 2012; Fryer et al., 1995; Hathorne et al., 2007; Jochum et al., 2012). Elemental fractionation is higher for smaller craters than for larger craters at constant sampling time. The choice of 65 µm crater sizes in this study presents a good compromise between maximal spatial resolution and at the same time minimal elemental fractionation for the lithophile elements. In fact, fractionation factors approach 1(i.e. no significant elemental fractionation) for lithophile elements for silicate glasses and carbonate reference materials at 65 µm crater size (Jochum et al., 2012).

2.4 Chronological development and growth

Seasonal changes in ambient temperature and light drive variability in *Clathromorphum* sp. growth rates throughout the year (Adey et al., Accepted). The physical differences between winter and summer cells were clearly visible in all specimens. Mg/Ca values measured along transects were visually matched with the changes in cell structure to develop annual chronologies for each specimen. Working from the youngest to the oldest part of the sampling path, years were assigned to each annual growth increment and the corresponding seasonal cycle of Mg/Ca in each specimen using the winter growth line to assign January for each year. Previous chronologies in several of the specimens were independently developed for growth-increment width analyses (Halfar et al., 2011b) and verified against those determined in the

current study. Additionally, the previous chronology for specimen 11-4 was verified using U/Th dating (Halfar et al., 2007). Annual growth rates were determined in specimen G1-1a by measuring the distance between winter growth lines. Annual growth rates for the remaining five specimens were previously measured by Halfar et al. (2011b) (Table 1). Analyseries software (Paillard et al., 1996) was used to assign the annual chronology to a calendar year using the maximum and minimum values as tie points and then was used to down sample and linearly interpolate the LA-ICP-MS Mg/Ca transect records to a monthly-resolved time series (Figure 5).

2.5 Data analysis

Prior to interpolation to monthly resolution, the quality of the data was verified to ensure no sampling or analytical inconsistencies. In rare cases, the destructive sampling during laser ablation broke through to a conceptacle below the surface of the thick section that was not visible in the photomosaic image. In these cases, the Mg/Ca ratios were elevated, thus the entire year was removed for that transect. Spikes in the raw Mg/Ca related to variability in the laser signal intensity were avoided (see raw data in Figure 5). Outliers defined as ±1.5 times the interquartile range of the raw LA-ICP-MS data were removed.

Assignment of annual chronology to winter growth lines is relatively straight forward, yet assignment of individual Mg/Ca determinations to a calendar date or month is not always clear. To avoid introducing uncertainties from subannual dating assignments, we used only the maximum and minimum Mg/Ca values representing summer SST highs and winter SST lows, respectively, for calibration of the Mg/Ca values to SST. Such practice is commonly used in coral-based calibration studies (Corrège, 2006). Mg/Ca determinations were not smoothed prior to selecting the maximum and minimum Mg/Ca values to prevent muting the seasonal range.

To assess intra- and inter-specimen variability, standard descriptive statistics for maxima and minima were calculated on an expanding scale for each transect, each specimen, and each island. General linear model (GLM) statistics investigated differences among transects, specimens, and islands using SAS software (SAS Institute Inc). The absolute difference was determined between two transects within the same specimen, between two specimens from the same island, and between records from different islands. Absolute difference quantifies the discrepancy between coeval algal Mg/Ca measurements (Eq. 1) (DeLong et al., 2013).

$$AD = |alga_1 - alga_2|/\sqrt{2} \qquad \text{(Eq. 1)}$$

In paleoclimate calibration studies, linear regression typically assumes error is equal (reduced major axis) or negligible for the independent regressor (ordinary least squares) when a single time series is used (York et al., 2004). Weighted least squares (WLS) regression (York et al., 2004) allows for the assignment of weights based on uncertainty when such assessments are possible. WLS was used to determine the relationship for maximum and minimum values of skeletal Mg/Ca with coeval OISST for the interval from 1982 to 2003 using code developed in MATLAB® (DeLong et al., 2007). Regression analysis was performed on an expanding scale for each transect, each specimen, each island, and of all the specimens by averaging respective maxima and minima for each time series. The weights for this expanding scale regression analysis were determined by assessing standard error for each Mg/Ca determination based on deviations between the determination and the average of those determinations. The weights for OISST are the reported error of 0.3°C for SST (Reynolds et al., 2002). The reconstruction error for Mg/Ca-SST (°C) was determined using standard error of regression (σ_R) where n is the number of observations.

$$\sigma_R = (\Sigma (SST_{Mg/Ca} - SST_{observed})^2 / (n - 2))^{1/2} \quad \text{(Eq. 2).}$$

Covariance is reported as Pearson Product Moment correlation coefficients. All significance testing assumes a 5% significance level.

Following standard practices for calibration and verification in climate reconstructions (Crowley et al., 1999; Fritts et al., 1979), we verified the Mg/Ca-SST developed with OISST for the period 1982 to 2003 with HadISST (Rayner et al., 2003) for the verification interval from 1960 to 1981 for island-specific calibrations and for a master record comprised of all six specimens.

3. RESULTS

3.1 Average skeletal Mg/Ca

Mg/Ca values were averaged for the 43-year analysis period for each transect to evaluate intra-specimen, inter-specimen, and inter-island variability. The average of Mg/Ca was lowest for the specimens from Amchitka Island and highest for the specimens from Attu Island, regardless if average was determined from raw data with outliers removed or from only the maximum and minimum Mg/Ca values (Figure 6).

Average Mg/Ca values varied significantly between two transects within a single specimen in only one case, specimen G1-1 (p=0.03, n=44) (Figure 6b). Average maximum Mg/Ca values differed significantly between the two transects within specimens 4-1 and 7-6 from Amchitka Island, 8-27 from Akun Island, and G1-1 from Attu Island (all p<0.0001, n=44 except 7-6, p=0.015) (Figure 7a). Average minimum Mg/Ca values differed significantly between the two transects within specimens 4-1 and 7-6 from

Amchitka Island, 8-27 from Akun Island, and G1-1 from Attu Island (all $p<0.0001$, n=44 except 4-1, $p=0.0015$) (Figure 7a). Average Mg/Ca values did not significantly vary between any two specimens from the same island. Average maximum Mg/Ca values significantly differed between specimens 11-4 and G1-1 at Attu Island and between specimens 8-24 and 8-27 at Akun Island (all $p<0.0001$, n=44). They did not differ significantly between specimens 4-1 and 7-6 at Amchitka Island ($p=0.12$, n=44). Average minimum Mg/Ca values did not significantly differ between any pair of specimens from the same island (Figure 7a).

After the two transects within a specimen were averaged together to create a single record for each specimen, Mg/Ca values for each pair of specimens from a single island were averaged to converge on a single value for each island (Figures 6c, 7b). The average Mg/Ca value varied significantly among the three islands ($p=0.044$ for Amchitka and Akun Island, $p<0.0001$ for Attu Island relative to the other two, all n=44) (Figure 6c). Average maximum and minimum Mg/Ca values varied significantly among all three islands (all $p<0.0001$ except minimum values between Amchitka and Attu Island which was $p=0.0005$, all n=44) (Figure 7b).

3.2 Variability in Mg/Ca time series

Annual growth rates did not vary significantly with minimum, maximum, or annually averaged Mg/Ca values for any of the specimens (see Table 1 for average annual growth rates for each specimen). Analysis of the replicated transects tested reproducibility of the Mg/Ca records within a specimen and between specimens. Within a specimen, the average of the absolute differences (avg_{AD}) between two transects was <1σ of the magnitude of maximum analytical precision (<0.011 mol/mol) (Figure S1a-c). In fact, the absolute difference between transects never exceeded ±1σ of the magnitude of maximum analytical precision (±0.011 mol/mol, magnitude 0.022 mol/mol) in specimens 7-6 from Amchitka Island and 8-24 from Akun Island (Figure S1a-c). The absolute difference exceeded 1σ for 1% and 6% of the measurements for specimens G1-1 and 11-4, respectively, at Attu Island, 7% of the measurements for 4-1 from Amchitka Island, and 3% of the measurements for 8-27 at Akun Island. There was no consistent period in time in which the absolute difference between transects within a specimen exceeded 1σ among the different specimens.

The avg_{AD} between the two specimens at a single island was <1σ of the magnitude of maximum analytical precision (<0.011 mol/mol) (Figure S1d). In fact, the absolute difference between two specimens from a single island never exceeded 1σ of the magnitude of maximum analytical precision (±0.011 mol/mol,

magnitude 0.022 mol/mol) for the specimens at Attu and Amchitka Islands and for only 6% of the measurements for the two specimens at Akun Island (Figure S1d).

The avg_{AD} of the averaged-island records was <1σ of maximum analytical precision (<0.011 mol/mol) between each of the islands (Figure 8). The averaged-island records were the most different between Attu and Amchitka Island, with 8% of the measurements exceeding 1σ. Further observation indicates that the largest difference between Mg/Ca values in the Attu and Amchitka Islands occurs during the summer months in which all of the maximum values for Attu Island were higher than those for Amchitka Island (Figure 8). The avg_{AD} of the averaged islands record was 0.017 mol/mol for summer months and 0.003 mol/mol for winter months. The same pattern was found when comparing records between Akun and Amchitka Islands (0.004 and 0.009 mol/mol for winter and summer months, respectively) and Akun and Attu Islands (0.005 and 0.008 mol/mol for winter and summer months, respectively).

3.3 Mg/Ca relationship with SST

Seasonal variability in SST drives fluctuations in Mg/Ca values (Figures S1 and 8), consistent with previous studies (Hetzinger et al., 2009; Hetzinger et al., 2011). Here, individual regression equations for skeletal Mg/Ca with OISST were generated for each specimen by combining the replicated transects, for each island, and for all three of the islands combined to a master time series (Table 2).

Averaging two specimens from a single island to create an island-specific record as well as averaging the island-specific records to create a master record increased the correlation between SST and skeletal Mg/Ca and reduced the standard error of regression by increasing the signal-to-noise ratio (Table 2). By combining records together, the error of regression was reduced from ±0.65 to 0.84°C for a single specimen to ±0.45°C for the master record. The ±0.45°C reconstruction error for the master record was less than the analytical error for a single Mg/Ca determination converted to ºC (±0.96°C determined by multiplying the maximum analytical error (0.11 mol/mol) by the slope of the master equation (87.53 °C/mol/mol)).

The difference in maximum Mg/Ca values among the islands (Figure 7) caused the Mg/Ca-SST relationships among the islands to vary (Table 2). The highest slope characterized the Mg/Ca-SST relationship at Amchitka Island and the lowest slope characterized the Mg/Ca-SST relationship at Attu Island (Figure 9). The slope for Akun Island fell in the middle, although the specimen-specific Mg/Ca-SST relationship for specimen 8-24 was lower than that for Amchitka Island.

3.4 Verification of Mg/Ca-SST relationship

The algal Mg/Ca values were converted to SST using the determined transfer functions (Table 2). The minimum and maximum algal-SST significantly correlated with HadISST record, such that the algal-SST explained between 95% and 98% of the variance in the HadISST record (Table 3).

The annually averaged master algal-SST record correlated significantly to the HadISST dataset (r^2=0.18, p=0.004, n=44) and air temperatures from Shemya Air Force base (52.72°N, 174.10°E) for the period from 1960 to 1990 (r^2=0.17, p=0.02, n=30, air temperature leads algal-SST by 1 year) (Figure 10). This relationship improved when the annually averaged algal-SST was correlated against minimum monthly Shemya air temperature (r^2=0.84, p<0.0001, n=30, air temperature leads algal-SST by 1 year). In addition, both the maximum and minimum algal-SSTs significantly correlated with the maximum summer and minimum winter HadISST (r^2=0.13, p=0.014, n=44 and r^2=0.15, p=0.011, n=43, respectively; algal-SST lags HadISST by 1 year for winter values) (Figure 11).

Using the maximum and minimum values as tie points, the raw LA-ICP-MS data were interpolated to monthly values and converted to temperature in °C. This monthly-interpolated algal-SST significantly correlated with monthly HadISST; however, explained less of the variance than the comparisons with only the maximum and minimum values (Figure 12a; Tables 3 and 4). For both the maximum and minimum values, and monthly values, the master record explained the highest amount of variance in the gridded-SST and had the lowest error of regression (Tables 3 and 4).

The months of the intra-annual SST varies between that of the algal-SST and the HadISST. Generally, one to two months represented the warm and cold seasons in the algal-SST while seasonal changes in SST were evenly spaced out over the year in the HadISST dataset (three months for the warm season and five months for the winter season) (Figure 12a). The anomalies smoothed with a 25-monthly running average varied significantly (r^2=0.38, p<0.0001, n=493, Figure 12b). The residuals of the algal-SST minus the HadISST indicate that the algal-SST systematically overestimated temperature during the winter months and underestimated temperature during the late spring and early summer months (Figure 12c). Monthly algal-SST and HadISST significantly correlated over the duration of the verification interval based on running correlation (r values between 0.52 and 0.88, Figure 12d).

The annual averages for the analysis period were determined from the monthly-interpolated values. Annual HadISST correlated significantly with algal-SST for the 43 year study period (Figure 12a, Table

5). When separated into the verification (1960–1981) and calibration (1982–2003) intervals, annual averaged HadISST only significantly correlated with minimum algal-SST (Table 5).

4. DISCUSSION

4.1. Variability in Mg/Ca values

Mg/Ca values varied between transects within a single specimen and between specimens from nearby locations, although absolute differences were largely within 1σ analytical uncertainty (Figure S1). Still, it is important to understand the sources of the variability present between transects and between specimens from the same island with the goal of improving reproducibility in future studies. Below we address the factors that could induce variability in the algal skeletal Mg/Ca outside of that generated by ambient SST, first exploring within specimen variability, followed by among specimen variability, and then among island variability.

Matrix effects in LA-ICP-MS between the carbonate skeleton and glass standard can vary by up to 10% from day to day (Hetzinger et al., 2011) potentially causing a significant difference in mean Mg/Ca values between transects analyzed on different days (difference of up to 0.02 mol/mol). Although the mean absolute difference between two transects within a single specimen never exceeded 0.011 mol/mol, this analytical uncertainty may explain some of the differences between replicate transects within a specimen, particularly in specimen G1-1a (Figure 6). Analytical uncertainty, however, does not explain the inter-annual variability between transects or between specimens (Figure S1).

Sampling resolution varied between transects within a specimen due to the indirect paths the laser ablation system sometimes took to avoid the conceptacles. This means that the replicated transects were not necessarily parallel at all times. If one transect crossed a single year of growth at an angle rather than directly across the year of growth, this first transect could have higher resolution and each LA-ICP-MS data point will span a shorter period in time. This is likely a negligible influence here as there are at least several thousand LA–ICP-MS data points going into each 43-year transect (e.g., Figure 5). Instead, the very high-resolution LA-ICP-MS measurements (generally less than ten microns per sequential increment) may capture ultra-structural scale heterogeneity in the skeletal architecture and geochemistry (Adey et al., Accepted), similar to that reported in scleractinian corals (e.g., Allison and Finch, 2004). This may reflect biological processes altering geochemistry during calcification (i.e., vital effects), which will influence the Mg/Ca ratios on ultra-structural scales and may drive some variability among transects within a single specimen. *C. nereostratum,* along with all high-Mg calcite organisms, increases the ratio of Mg to Ca during calcification relative to that of seawater (Moberly, 1968) indicating that there is a vital

offset from seawater composition (Hetzinger et al., 2009). However, while calibration studies under controlled conditions using *C. nereostratum* are currently not available, the vital offset in Mg/Ca from seawater composition in this alga, similar to other organisms with a vital effect, is likely constant within a given species on the larger scales explored here, and does not drive variability among islands. The absence of significant influence of growth rates on Mg/Ca values on interannual timescales supports this assumption, as vital effects are largely associated with changes in calcification and linear extension (i.e., growth) rates. The absence of such a relationship between growth rates and Mg content is not consistent with previous studies that did not include *C. nereostratum* reporting that growth rates positively influence magnesium content in some species of coralline algae (Kolesar, 1978; Moberly, 1968).

Destructive invertebrate grazing on *C. nereostratum* continuously removes the outer layer of photosynthetic epithallium in *C. nereostratum* (Steneck, 1982) that covers the meristem cell layer (site of calcification) and the deeper basal perithallium forming the bulk of the plant. The perithallium is largely preserved without alteration after formation, the exception being dissolution of select parts of the skeleton due to the formation of conceptacles for reproduction and possible grazing extending beyond the epithallium into the perithallium. Uneven grazing could remove part or all of the previous year's growth at specific sites in the algal skeleton. Grazing would not remove an entire year of growth uniformly across the entire specimen. Careful selection of the LA-ICP-MS laser path using the digital images avoided sections of the skeleton showing signs of grazing. In areas where grazing removed part of the previous year's growth, the growth band in the skeleton would still be present but part of the year's growth would be absent or filled with specialized cells formed by the algae to repair the wound post-grazing (hypothallium). Grazing may be more evident during warmer summer temperatures when invertebrates are more active, resulting in the removal of skeleton containing maximum Mg/Ca values. Consequently, reconstructed algal-SSTs would underestimate actual SST values. Although grazed areas visible in the digital images were avoided during analyses of the specimens here, it is feasible that small amounts of grazed material were missing from the analyzed material resulting in the wider variability present in the reconstructed summer SSTs. Collecting specimens from colder water deeper in the water column (>10 m) may reduce the influence of grazers, although these algae would be more likely to capture changes in the subsurface water temperature and not SST.

Temperature and light levels influence Mg/Ca in other coralline algae (Moberly 1968). Therefore, specimen-specific habitat characteristics including different light levels may drive the Mg/Ca variability between specimens of *C. nereostratum* at a single island. This variability in Mg/Ca values was most evident between the two samples from Akun Island (Figure S1d). The rocky bottom of Akun Island has a

small scale (<50 cm) spur and groove morphology and light levels reaching the two specimens oriented differently toward the light within this habitat structure may have differed over the lifespans, resulting in offsets in Mg/Ca between the two specimens. Regardless of the cause of the variability, we can make the broad assumption that the average of the two samples starts to converge on a single value representative of each island. To support this assumption, we find that the average absolute difference between two specimens at the same island is either similar to or lower than the difference between two transects within a single specimen (Figure S1).

The largest differences among the islands occur during the summer months (Figures 8 and 9). While maximum monthly SSTs varied among the islands (Figure 4), this difference was not large enough to explain the variability in maximum monthly Mg/Ca. The long residence time of Mg and Ca in seawater (Lear et al., 2002) suggests that there is little variability in seawater Mg/Ca between islands. Therefore, this is not a contributor to the significant variability that exists between islands, although without local seawater measurements there is the possibility that site-specific mixing or upwelling could alter the local saturation state with respect to high-Mg calcite. These island-specific effects indicate that, if available, local SST-Mg/Ca calibrations are preferred to reconstruct summer SST.

4.2 Verification of Mg/Ca-SST transfer functions

This study does not evaluate the fidelity of gridded-SST data in reflecting *in situ* seawater temperature at the sites that the coralline algae were collected from. This is important to note as the thermocline can shoal to less than 10 m in the Aleutian archipelago during the summer season (Callaway, 1963) bathing the algae in cooler water. Thus, local shoaling/upwelling of colder deep waters may drive the deviations of the algal-SST from the gridded-SST dataset (Figure 12a). Correlations between the algal-derived SST and observed seawater temperature may improve when Mg/Ca values are compared to *in situ* seawater temperature. Collecting specimens from sites with local measurements thus needs to be prioritized for future studies.

In comparing annual average SSTs averaged for the 43 year analysis period, the average determined by only maximum and minimum values (HadISST average = 6.4°C and algal-SST average = 6.5°C) overestimated HadISST determined from monthly values (5.8°C). This results from a longer winter season than summer season in the Aleutian archipelago (i.e., there are five cold months and only three warm months (Figure 12a)). Using an annual average of only two values, a single maximum value to represent the summer and a single value minimum value to represent the winter thus underrepresents the cold months. However, the transfer function developed here can be applied to interpolated values to

reconstruct monthly SSTs (Figure 12a). The deviation of the shape of the monthly-interpolated algal-SST values differs from the monthly HadISST values (Figure 12a), which is evident in the cyclical residuals (Figure 12c), suggests the assignment of monthly Mg/Ca introduced subannual dating uncertainties. Assuming that *in situ* temperatures follow a smooth seasonal cycle, these data indicate that algal growth is slow during the cold winter and warm summer months during the year, and faster during the spring and fall months (Figure 12a). This is not consistent with faster summer growth in *C. compactum* (Adey, 1965; Halfar et al., 2008). Thus, the intra-annual deviations in the algal record from HadISST may reflect changes in thermocline shoaling. Regardless, the 43-year average of the monthly-interpolated algal-SST values (6.2°C) overestimates HadISST determined from monthly values (5.8°C) by 0.4°C, which is less than the error of regression for the master record (±0.45°C).

The annually averaged algal-SSTs captured the HadISST records well over the 43 years of the study period, although annually-averaged Mg/Ca explains a relatively small amount of SST variance on inter-annual timescales (Table 5, Figures 10). The low variability in SST from year to year (largely <1°C), which often does not exceed the error of the Mg/Ca-SST regression (1σ magnitude = 0.9°C), could drive the small amount of variance captured. The algal Mg/Ca-SST record will capture a larger percentage of variability in SST when that variability exceeds the error regression, which may be expected to occur on longer timescales. The HadISST values correlated the strongest with the winter algal-SST values and the weakest with the summer algal-SST values (Table 5), likely reflecting the larger analytical error during measurement of higher Mg/Ca values, the increased grazing from chitons during the summer, and potentially a greater influence of light variability during the summer season. In addition, the algal-SST records of summer values and winter values both followed changes in minimum and maximum HadISST (Figure 11), allowing the algal Mg/Ca values to be a tool to reconstruct past seasonality. In some cases, the algal Mg/Ca-SST lagged air temperature by one year (Figure 10, Table 5). This lag could reflect inaccuracies of the chronology but more likely, rounding error resulting from subannual dating uncertainties. Improved understanding of intra-annual growth rates in the algae would work to address this problem.

4.3 Summary

The long-lived coralline algae *C. nereostratum* may start to address the data gap in high-resolution proxy archives of mid-to-high latitude climate variability. Replicated skeletal Mg/Ca values from multiple specimens from three islands in the Aleutian archipelago displayed island-specific variability during the summer months. As a result, island-specific calibrations were generated to convert the skeletal Mg/Ca of six specimens to SST and then combined to generate a regional reconstruction of algal-SST, with an error

of ±0.45°C. Thus, using replicated Mg/Ca-derived SST reconstructions from the coralline algae, both absolute changes in past seawater temperature variability as well as seasonality in the Aleutian archipelago can be assessed. These reconstructions are particularly significant because of the strong anthropogenic alteration projected for the northern North Pacific Ocean and Bering Sea.

ACKNOWLEDGEMENTS

This research was funded by Natural Sciences and Engineering Research Council of Canada (NSERC) Discovery and Ship Time Grants to JH. SH was funded by the Alexander von Humboldt Foundation (Feodor Lynen Fellowship). NOAA/OAR/ESRL PSD, Boulder, Colorado, USA provided the NOAA_OI_SST_V2 data. The Met Office Hadley Center provided the HadISST data.

BIBLIOGRAPHY

Adey, W., 1965. The genus Clathromorphum (Corallinaceae) in the Gulf of Maine. Hydrobiologia 26, 539-573.

Adey, W., Halfar, J., Williams, B., Accepted. Biological, physiological and ecological factors controlling high magnesium carbonate formation and producing a precision Arctic/Subarctic marine climate archive: the coralline genus *Clathromorphum* Foslie emend Adey. Smithsonian Contributions to the Marine Sciences.

Black, B., Copenheaver, C., Frank, D., Stuckey, M., Kormanyos, R., 2009. Multi-proxy reconstructions of northeastern Pacific sea surface temperature data from trees and Pacific geoduck. Palaeogeography, Palaeoclimatology, Palaeoecology 278, 40-47.

Bourassa, M., Gille, S., Bitz, C., Carlson, D., Cerovecki, I., Clayson, C., Cronin, M., Drennan, W., Fairall, C., Hoffman, R., Magnusdottir, G., Pinker, R., Renfrew, I., Serreze, M., Speer, K., Talley, L., Wick, G., 2013. High-latitude ocean and sea ice surface fluxes: challenges for climate research Bulletin of the American Meteorological Society 94, 403-423.

Callaway, R., 1963. Ocean conditions in the vicinity of the Aleutian Islands, Summer 1957, International North Pacific Fisheries Commission Series, p. 156.

Chan, P., Halfar, J., Williams, B., Hetzinger, S., Steneck, R., Zack, T., Jacob, D., 2011. Freshening of the Alaska Coastal Current recorded by coralline algal Ba/Ca ratios. Journal of Geophysical Research 116, G01032, doi:01010.01029/02010JG001548.

Corrège, T., 2006. Sea surface temperature and salinity reconstruction from coral geochemical tracers. Palaeogeography, Palaeoclimatology, Palaeoecology 232, 408-428.

Crowley, T., Quinn, T., Hyde, W., 1999. Validation of coral temperature calibrations. Paleoceanography 14, 605-615, doi:610.1029/1999PA900032.

Czas, J., Jochum, K., Stoll, B., Weis, U., Yang, Q.-C., Jacob, D., Andreae, M., 2012. Investigation of matrix effects in 193 nm LA-ICP-MS analysis using reference glasses of different transparencies. Spectrochimica Acta Part B 78, 20-28.

de Villiers, S., Nelson, B., Chivas, A., 1995. Biological controls on coral Sr/Ca and $\delta^{18}O$ reconstructions of sea surface temperatures. Science 269, 1247-1249.

DeLong, K., Quinn, T., Taylor, F., 2007. Reconstructing twentieth-century sea surface temperature variability in the southwest Pacific: A replication study using multiple coral Sr/Ca records from New Caledonia. Paleoceanography 22, PA4212, doi:4210.1029/2007PA001444.

DeLong, K., Quinn, T., Taylor, F., Shen, C.-C., Lin, K., 2013. Improving coral-base paleoclimate reconstructions by replicating 350 years of coral Sr/Ca variations. Palaeogeography, Palaeoclimatology, Palaeoecology 373, 6-24.

Deser, C., Alexander, M., Xie, S.-P., Phillips, A., 2010. Sea surface temperature variability: patterns and mechanisms. Annual Review of Marine Science 2, 115-143, doi:110.1146/annurev-marine-120408-151453.

Fritts, H., Lofgren, G., Gordon, G., 1979. Variations in climate since 1602 as reconstructed from tree rings. Quaternary Research 12, 18-46.

Fryer, B., Jackson, S., Longerich, H., 1995. The design, operation and role of the laser-ablations microprobe coupled with an inductively coupled plasma-mass spectrometer (LAM-ICP-MS) in the Earth sciences. The Canadian Mineralogist 33, 303-312.

Gregory, J.M., Bi, D., Collier, M.A., Dix, M.R., Hirst, A.C., Hu, A., Huber, M., Knutti, R., Marsland, S.J., Meinshausen, M., Rashid, H.A., Rotstayn, L.D., Schurer, A., Church, J.A., 2013. Climate models without preindustrial volcanic forcing underestimate historical ocean thermal expansion. Geophysical Research Letters 40, 1600-1604.

Halfar, J., Adey, W., Kronz, A., Hetzinger, S., Edinger, E., Fitzhugh, W., 2013. Arctic sea-ice decline archived by multicentury annual-resolution record from crustose coralline algal proxy. Proceedings of the National Academy of Sciences, doi: 10.1073/pnas.1313775110.

Halfar, J., Hetzinger, S., Adey, W., Zack, T., Gamboa, G., Kunz, B., Williams, B., Jacob, D., 2011a. Coralline algal growth-increment widths archive North Atlantic climate variability. Palaeogeography, Palaeoclimatology, Palaeoecology 302, 71-80, doi:10.1016/j.palaeo.2010.1004.1009.

Halfar, J., Steneck, R., Joachimski, M., Kronz, A., Wanamaker Jr., A., 2008. Coralline red algae as high-resolution climate recorders. Geology 36, 463-466, doi: 410.1130/G24635A.24631.

Halfar, J., Steneck, R., Schone, B., Moore, G., Joachimski, M., Kronz, A., Fietzke, J., Estes, J., 2007. Coralline alga reveals first marine record of subarctic North Pacific climate change. Geophysical Research Letters 34, L07702, doi:07710.01029/02006GL028811.

Halfar, J., Williams, B., Hetzinger, S., Steneck, R., Lebednik, P., Winsborough, C., Omar, A., Chan, P., Wanamaker Jr., A., 2011b. 225 years of Bering Sea climate and ecosystem dynamics revealed by coralline algal growth-increment widths. Geology 39, 579-582, doi: 510.1130/G31996.31991.

Hathorne, E., James, R., Savage, P., Alard, O., 2007. Physical and chemical characteristics of particles produced by laser ablation of biogenic calcium carbonate. Journal of Analytical Atomic Spectrometry 23, 240-243.

Hetzinger, S., Halfar, J., Kronz, A., Steneck, R., Adey, W., Lebednik, P., Schone, B., 2009. High-resolution Mg/Ca ratios in a coralline red alga as a proxy for Bering Sea temperature variations from 1902 to 1967. Palaios 24, 406-412, doi: 410.2110/palo.2008.p2108-2116r.

Hetzinger, S., Halfar, J., Mecking, J., Keenlyside, N., Kronz, A., Steneck, R., Adey, W., Lebednik, P., 2012. Marine proxy evidence linking decadal North Pacific and Atlantic climate. Climate Dynamics, doi: 10.1007/s00382-00011-01229-00384.

Hetzinger, S., Halfar, J., Zack, T., Gamboa, G., Jacob, D., Kunz, B., Kronz, A., Adey, W., Lebednik, P., Steneck, R., 2011. High-resolution analysis of trace elements in crustose coralline algae from the North Atlantic and North Pacific by laser ablation ICP-MS. Palaeogeography, Palaeoclimatology, Palaeoecology 302, 81-94.

Hetzinger, S., Halfar, J., Zack, T., Mecking, J., Kunz, B., Jacob, D., Adey, W., 2013. Coralline algal Barium as indicator for 20th century northwestern North Atlantic surface ocean freshwater variability. Scientific Reports 3, 1761, doi:1710.1038/srep01761.

IPCC, 2013. IPCC, 2013: Summary for Policymakers. In: Climate Change 2013: The Physical Science Basis., in: Stocker, T.F., D. Qin, G.-K. Plattner, M. Tignor, S. K. Allen, J. Boschung, A. Nauels, Y. Xia, V. Bex and P.M. Midgley (Ed.), Contribution of Working Group I to the Fifth Assessment Report of the Intergovernmental Panel on Climate Change, Cambridge, United Kingdom and New York, NY, USA.

Jacob, D., 2006. High sensitivity analysis of trace element poor geological reference glasses by laser-ablation inductively coupled plasma mass spectrometry (LAICP-MS). Geostandards and Geoanalytical Research 30, 221-235.

Jochum, K., Nohl, U., Herwig, K., Lammel, E., Stoll, B., Hofmann, A., 2005. GeoReM: A new geochemical database for reference materials and isotopic standards. Geostandards and Geoanalytical Research 29, 333-338.

Jochum, K., Scholz, D., Stoll, B., Weis, U., Wilson, S., Yang, Q., Schwalb, A., Börner, N., Jacob, D., Andreae, M., 2012. Accurate trace element analysis of speleothems and biogenic calcium carbonates by LA-ICP-MS. Chemical Geology 2012.

Kaplan, A., Cane, M., Kushnir, Y., Clement, A., Blumenthal, M., Rajagopalan, B., 1998. Analyses of global sea surface temperature 1856-1991. Journal of Geophysical Research 103, 18,567-518,589.

Kolesar, P., 1978. Magnesium in calcite from a coralline alga. Journal of Sedimentary Petrology 48, 815.

Lamb, H.H., 1965. The early medieval warm epoch and its sequel. Palaeogeography, Palaeoclimatology, Palaeoecology 1, 13-37.

Lamb, H.H.S., N. J.; Worssam, B. C.; Hodgson, J. M.; A. R., Lord; Shotton, F. W.; Schove, D. J.; Cooper, L. H. N., 1977. The Oxygen Isotope Stratigraphic Record of the Late Pleistocene:

Discussion. Philosophical Transactions of the Royal Society of London. Series B, Biological Sciences 280, 179-182.

Lear, C., Rosenthal, Y., Slowey, N., 2002. Benthic foraminiferal Mg/Ca-paleothermometry: A revised core-top calibration. Geochimica et Cosmochimica Acta 66, 3375-3387.

Meehl, G., Washington, W., Santer, B., Collins, W., Arblaster, J., Hu, A., Lawrence, D., Teng, H., Buja, L., Strand, W., 2006. Climate Change Projections for the Twenty-First Century and Climate Change Commitment in the CCSM3. Journal of Climate 19, 2597-2616.

Moberly, R., 1968. Composition of magnesian calcites of algae and pelecypods by electron microprobe analysis. Sedimentology 11, 61-82.

Paillard, D., Labeyrie, L., Yiou, P., 1996. Macintosh program performs timeseries analysis. EOS, Transactions, American Geophysical Union 77, 379.

Pearce, N., Perkins, W., Westgate, J., Gorton, M., Jackson, S., Neal, C., Chenery, S., 1997. A compilation of new and published major and trace element data for NIST SRM 610 and NIST SRM 612 glass reference materials. Geostandards Newsletter 21, 115-144.

Rayner, N., Parker, D., Horton, E., Folland, C., Alexander, L., Rowell, D., 2003. Global analyses of sea surface temperature, sea ice, and night marine air temperature since the late nineteenth century. Journal of Geophysical Research 108, 4407, doi:4410.1029/2002JD002670.

Reed, R., Stabeno, P., 1994. Flow along and across the Aleutian Ridge. Journal of Marine Research 52, 639-648.

Reynolds, R., Rayner, N., Smith, T., Stokes, D., Wang, W., 2002. An improved in situ and satellite SST analysis for climate. Journal of Climate 15, 1609-1625.

Reynolds, R., Smith, T., 1994. Improved Global Sea Surface Temperature Analyses Using Optimum Interpolation. Journal of Climate 7, 929-948.

Slutz, R., Lubker, S., Hiscox, J., Woodruff, S., Jenne, R., Joseph, D., Steuer, P., Elms, J., 1985. Comprehensive Ocean-Atmosphere Data Set: Release 1. Climate Research Program, Boulder, Colorado.

Smith, T., Reynolds, R., 2004. Improved extended reconstruction of SST (1854-1997). Journal of Climate 17, 2466-2477.

Solomon, S., Qin, D., Manning, M., Alley, R., Berntsen, T., Bindoff, N., Chen, Z., Chidthaisong, A., Gregory, J., Hegerl, G., Heimann, M., Hewitson, B., Hoskins, B., Joos, F., Jouzel, J., Kattsov, V., Lohmann, U., Matsuno, T., Molina, M., Nicholls, N., Overpeck, J., Raga, G., Ramaswamy, V., Ren, J., Rusticucci, M., Somerville, R., Stocker, T., Whetton, P., Wood, R., Wratt, D., 2007. Technical Summary. In: Climate Change 2007: The Physical Science Basis. Contribution of Working Group I to the Fourth Assessment Report of the Intergovernmental Panel on Climate Change, in: Solomon, S., Qin, D., Manning, M., Chen, Z., Marquis, M., Averyt, K., Tignor, M., Miller, H. (Eds.), Cambridge University Press, Cambridge, United Kingdom and New York, NY, USA.

Steneck, R., 1982. A limpet-coralline alga association: adaptations and defenses between a selective herbivore and its prey. Ecology 63, 507-522.

Torres, M., Zima, D., Falkner, K., Macdonald, R., O'Brien, M., Schöne, B., Siferd, T., 2011. Hydrographic Changes in Nares Strait (Canadian Arctic Archipelago) in Recent Decades Based on $\delta^{18}O$ Profiles of Bivalve Shells. Arctic 64, 45-58.

Williams, B., Halfar, J., Steneck, R., Wortmann, U., Hetzinger, S., Adey, W., Lebednik, P., Joachimski, M., 2011. Twentieth century $\square^{13}C$ variability in surface water dissolved inorganic carbon recorded by coralline algae in the northern North Pacific Ocean and the Bering Sea. Biogeosciences 8, 165-174, doi:110.5194/bg-5198-5165-2011.

Worley, S., Woodruff, S., Reynolds, R., Lubker, S., Lott, N., 2005. ICOADS release 2.1 data and products. International Journal of Climatology 25, 823-842, doi: 810.1002/joc.1166.

York, D., Evensen, N., Lopez Martinez, M., De Basabe Delgado, J., 2004. Unified equations for the slope, intercept, and standard errors of the best straight line. American Journal of Physics 72, 367-375.

TABLE CAPTIONS

Table 1. Locations and average annual growth rates of *C. nereostratum* specimens.

Table 2. Weighted least squares (WLS) linear regression coefficients for Mg/Ca to SST determined for the interval from 1982 to 2003. Monthly Mg/Ca is independent regressor (X-axis) and monthly SST is the dependant (Y-axis). Reported errors are 1σ. R is the Pearson Product Moment correlation coefficient and σ_R is the standard error of regression in°C. Units are °C for the intercept and °C/mol/mol for the slope.

Table 3. Comparison of algal-SST with HadISST maximum and minimum values for the calibration (1982-2003) and verification intervals (1960-1981). σ_R is the error of regression.

Table 4. Comparison of monthly-interpolated algal-SST with monthly HadISST values for the interval 1960-2003. σ_R is the error of regression.

Table 5. Comparison of algal-SST and HadISST for the annual minimum, annually averaged from monthly-interpolated values, and annual maximum values for the entire analysis period (winter 1960 to summer 2003), the verification interval (winter 1960 to summer 1981) and calibration interval (winter 1982 to summer 2003). Statistically significant relationships are highlighted.

FIGURE CAPTIONS

Figure 1. (A) Specimen collected from Attu Island showing tissue and gross skeletal structure; hammer shown for scale (B) Polished thick slab of sectioned specimen with parallel laser tracks from the LA-ICP-MS. The black holes in B are the conceptacles which formerly contained the reproduction structures.

Figure 2. Sites of *C. nereostratum* collection (Table 1) in the Aleutian archipelago. Arrows indicate pathway of Alaskan Stream.

Figure 3. (A) Comparison of annually averaged HadISST (black line) (Rayner et al., 2003), ERSST (green line) (Smith and Reynolds, 2004), COADS (red line) (Worley et al., 2005), and satellite-derived SST from NOAA OISST (bold grey line, left axis) (Reynolds et al., 2002) for the grid encompassing the Aleutian archipelago (approximately 50°N to 56°N by 172°E to 165°W, depending on the data product). (B) Number (#) of ICOADS observations (Slutz et al., 1985) per year for the same grid area as in A.

Figure 4. Average maximum and minimum monthly (±1σ) gridded SSTs from the (A) HadISST dataset (Rayner et al., 2003) and (B) OISST dataset (Reynolds et al., 2002) for the 1°x1° grid encompassing Attu Island (grey circle), Amchitka Island (white square), and Akun Island (black triangle) for the period from 1982 to 2003. (C) Time series of monthly gridded-SST from the OISST dataset and annual averages (bold lines) for Attu Island (grey), Amchitka Island (dashed), and Akun Island (black); symbols same as (A) and (B).

Figure 5. Ten years of raw LA-ICP-MS data (light grey line) and monthly-interpolated data (black line) for specimen 11-4 from Attu Island. Error bars represent analytical precision (2σ).

Figure 6. Average Mg/Ca value (±1σ) for the period 1960-2003 for each transect (grey) and specimen (black) for specimens from Attu (circles), Amchitka (squares), and Akun (triangles) Islands for (A) the raw LA-ICP-MS data with outliers removed, (B) the data determined from only the maximum and minimum values, and (C) averages for each island. Analytical uncertainty for averaged values was 0.0085 mol/mol. The error bar represents analytical precision (2σ).

Figure 7. (A) Average maximum and minimum Mg/Ca values (±1σ) for each transect (grey) and specimen (black; average of transects) from Attu, Amchikta, and Akun Islands. (B) Average (±1σ)

maximum and minimum Mg/Ca values for each Island. (All the averages are for the period of 1960 to 2003. Error bars represent analytical precision (2σ).

Figure 8. Minimum and maximum, and annual averages (bold line) derived from the maximum and minimum Mg/Ca values (mol/mol) for each island. Error bars represent analytical precision (2σ). (line plot) Absolute difference between Attu and Akun Islands (light grey), Amchitka and Akun Islands (dark grey), and Attu and Amchitka Islands (black) (area plot).

Figure 9. Calibration of algal Mg/Ca with OISST determined using WLS (r=0.95, 0.97, 0.96 for Amchitka, Attu and Akun Islands, respectively, p<0.05 and n=44 for each island). The shaded region is 95% confidence band for each regression.

Figure 10. Annually averaged (bold line) algal-SST (black with σ_R of ±0.45°C error in shaded light grey), HadISST (grey), and Shemya air temperature (dashed). SST annual averages were derived from the maximum and minimum values.

Figure 12. Maximum and minimum algal-SST (black) and HadISST (grey).

Figure 12. (A) Comparison of monthly-interpolated and 25-month running average (bold line) algal-SST values with HadISST. (B) Anomalies from (A). (C) Residuals of the algal-SST minus the HadISST. (D) Running correlation (25-month) between algal-SST and HadISST.

SUPPLEMENTAL FIGURE

Supplemental Figure 1. Maximum and minimum and annual averages (bold line) derived from the maximum and minimum Mg/Ca values (mol/mol) for each transect for each specimen (A-C) and the average of each transect for each specimen (D) (line plots). Also plotted is the absolute difference between the two transects for the maximum and minimum values (area plots). Error bars represent analytical precision (2σ).

Table 1

Island	Specimen	Latitude, Longitude	Collection Date	Average annual growth rates (μm yr^{-1})
Amchitka	4-1	51°25.57N, 179°14.27E	August 2004	342
	7-6	51°24.54N, 179°23.01E	August 2004	464
Attu	G1-1a	52°56.02N, 173°15.97E	June 2008	542
	11-4	52°47.79N, 173°10.77E	August 2004	379
Akun	8-27	54°12.94N, 165°30.85W	June 2008	450
	8-24	54°12.94N, 165°30.85W	June 2008	414

Table 2

		Intercept		Slope		R	σ_R	N
Attu	G1-1a	-5.41	±0.26	80.37	±1.76	0.98	0.65	44
	11-4	-5.46	±0.23	85.17	±1.58	0.98	0.68	44
	Island average	-5.41	±0.23	83.10	±1.59	0.99	0.58	44
Amchitka	4-1	-7.02	±0.38	105.77	±3.34	0.97	0.77	44
	7-6	-7.07	±0.36	103.67	±2.60	0.97	0.73	44
	Island average	-6.55	±0.26	100.46	±1.97	0.97	0.70	44
Akun	8-24	-3.54	±0.21	74.88	±1.50	0.97	0.84	44
	8-27	-5.94	±0.27	97.77	±2.10	0.98	0.74	44
	Island average	-5.19	±0.24	90.18	±1.95	0.98	0.70	44
Master		-5.46	±0.36	87.53	±3.05	0.99	0.45	44

Table 3

	Calibration (1982-2003)	Verification (1960-1981)
Attu Island	r^2=0.98, p<0.0001, n=44, σ_R=0.52	r^2=0.97, p<0.0001, n=44, σ_R=0.63
Amchitka Island	r^2=0.97, p<0.0001, n=44, σ_R=0.55	r^2=0.95, p<0.0001, n=44, σ_R=0.64
Akun Island	r^2=0.96, p<0.0001, n=44, σ_R=0.74	r^2=0.95, p<0.0001, n=44, σ_R=0.76
Master	r^2=0.98, p<0.0001, n=44, σ_R=0.43	r^2=0.98, p<0.0001, n=44, σ_R=0.51

Table 4

	Interval 1960-2003
Attu Island	r^2=0.45, p<0.0001, n=517, σ_R=1.30
Amchitka Island	r^2=0.44, p<0.0001, n=517, σ_R=1.08
Akun Island	r^2=0.39, p<0.0001, n=517, σ_R=1.42
Master	r^2=0.50, p<0.0001, n=517, σ_R=1.07

Table 5

	Algal-SST minimum	Algal-SST annual	Algal-SST maximum
1960-2003			
HadISST min	r^2=0.15, p=0.011, n=43*	r^2=0.21, p=0.002, n=44	r^2=0.17, p=0.005, n=44
HadISST annual	r^2=0.46 p<0.0001, n=43*	r^2=0.27, p=0.0003, n=44	r^2=0.28, p=0.0002, n=44
HadISST max	r^2=0.35, p<0.0001, n=43*	r^2=0.10, p=0.042, n=44	r^2=0.13, p=0.014, n=44
1961-1981			
HadISST min	r^2=0.03, p=0.46, n=22*	r^2=0.006, p=0.72, n=22	r^2=0.03, p=0.48, n=22
HadISST annual	r^2=0.50, p=0.0002, n=22*	r^2=0.14, p=0.08, n=22	r^2=0.17, p=0.06, n=22
HadISST max	r^2=0.44, p=0.0007, n=22*	r^2=0.10, p=0.15, n=22	r^2=0.14, p=0.08, n=22
1982-2002			
HadISST min	r^2=0.07, p=0.24, n=21*	r^2=0.08, p=0.21, n=22	r^2=0.03, p=0.42, n=22
HadISST annual	r^2=0.22, p=0.030, n=21*	r^2=0.02, p=0.57, n=22	r^2=0.02, p=0.49, n=22
HadISST max	r^2=0.19, p=0.050, n=21*	r^2=0.006, p=0.74, n=22	r^2=0.002, p=0.84, n=22

*Alga lags HadISST by 1 year

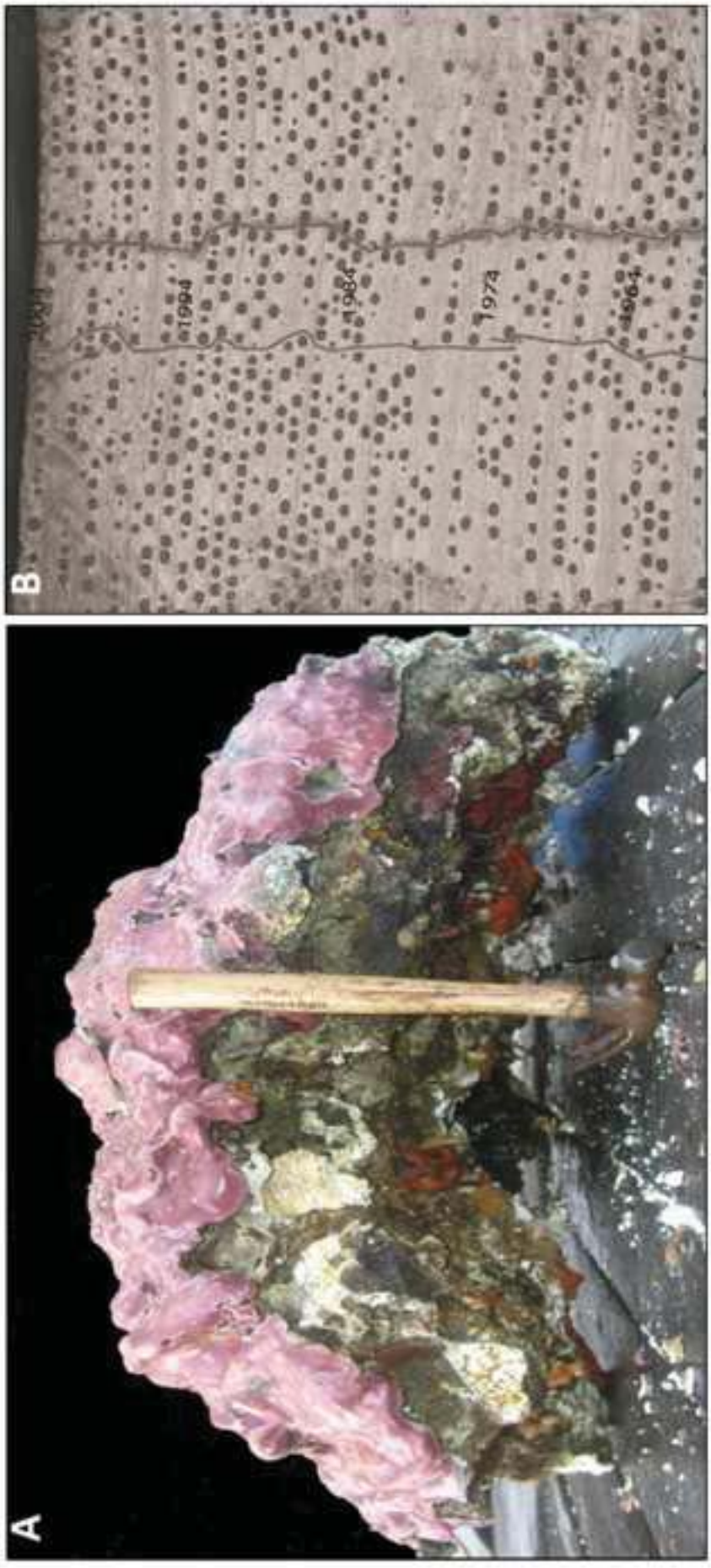

Figure 1

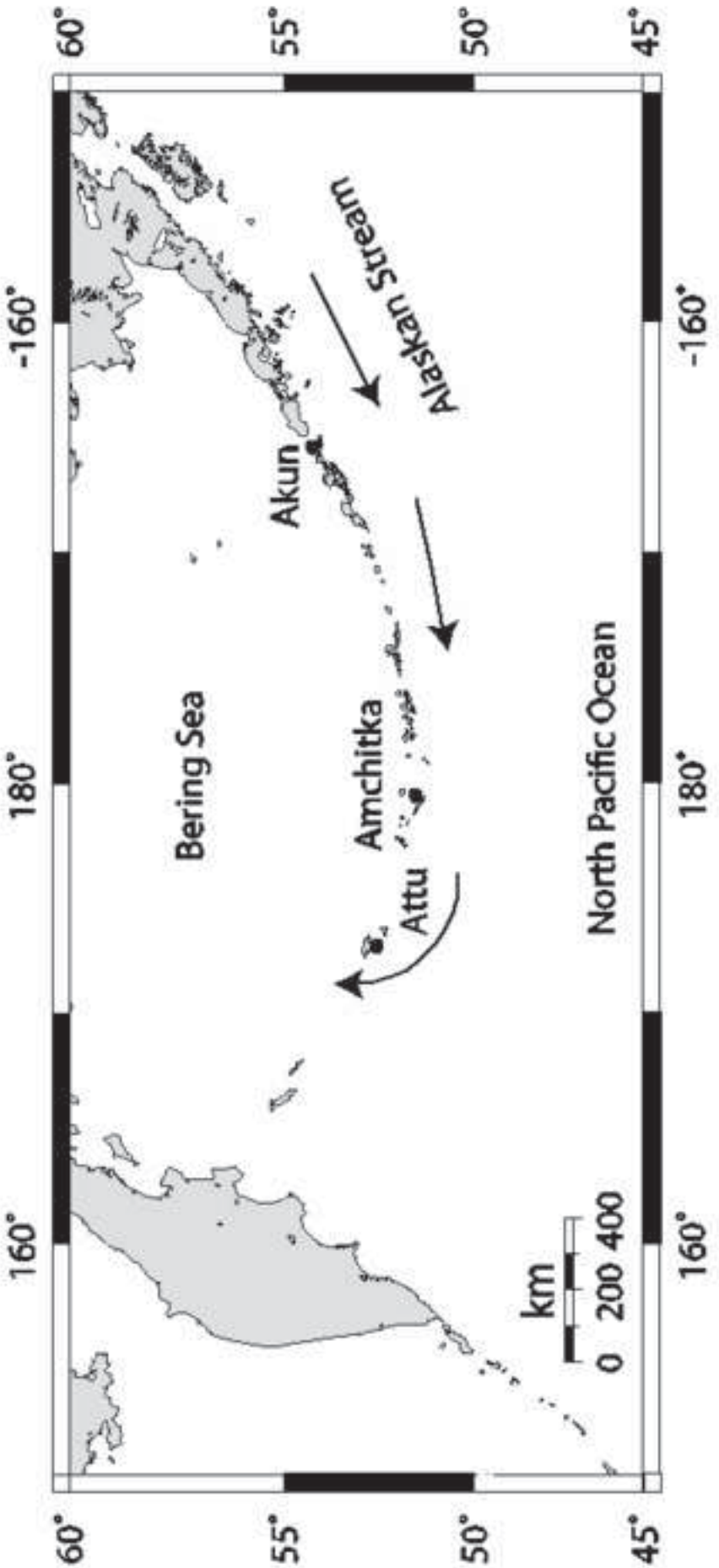

Figure 2

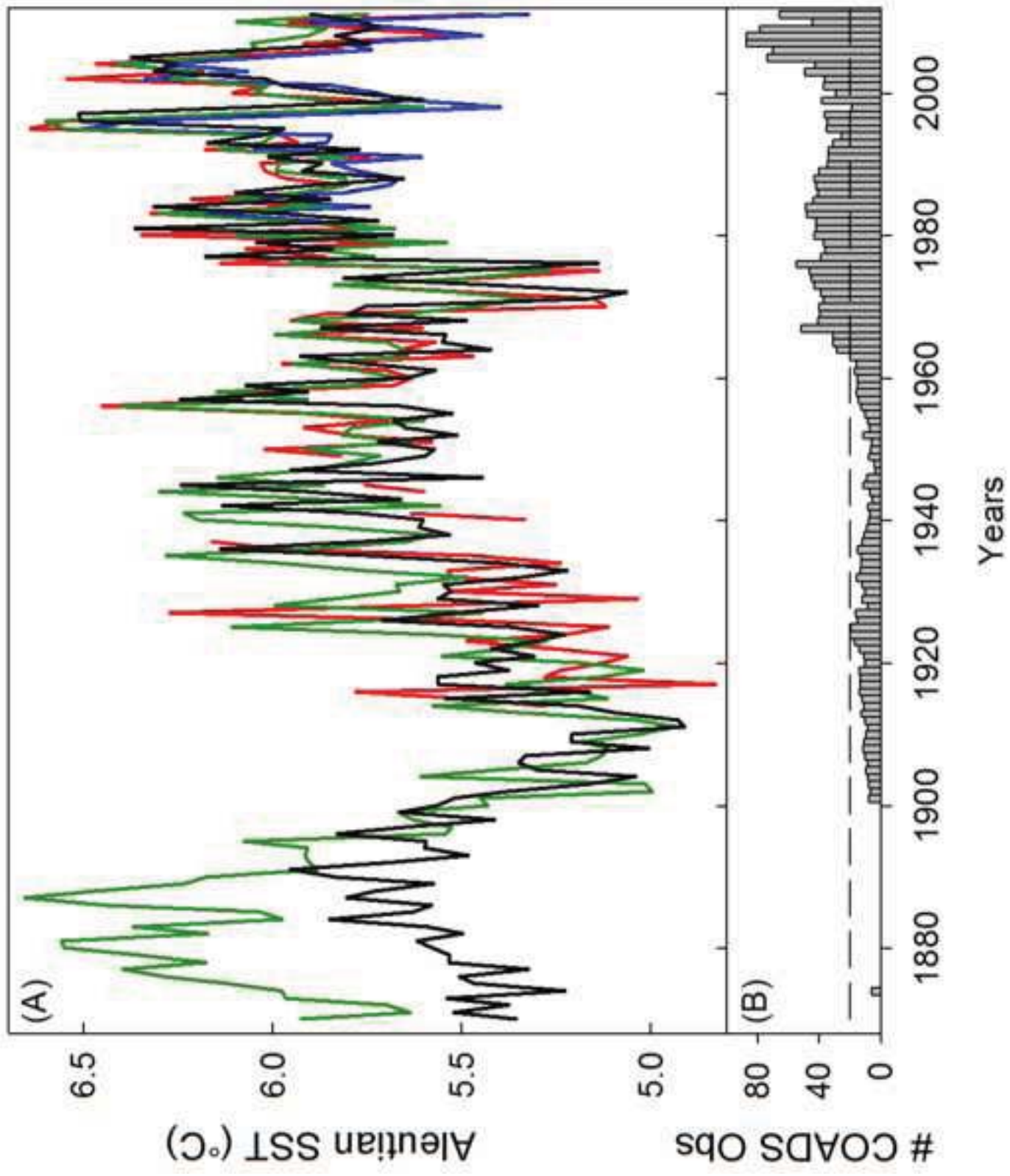

Figure 3

Figure 4

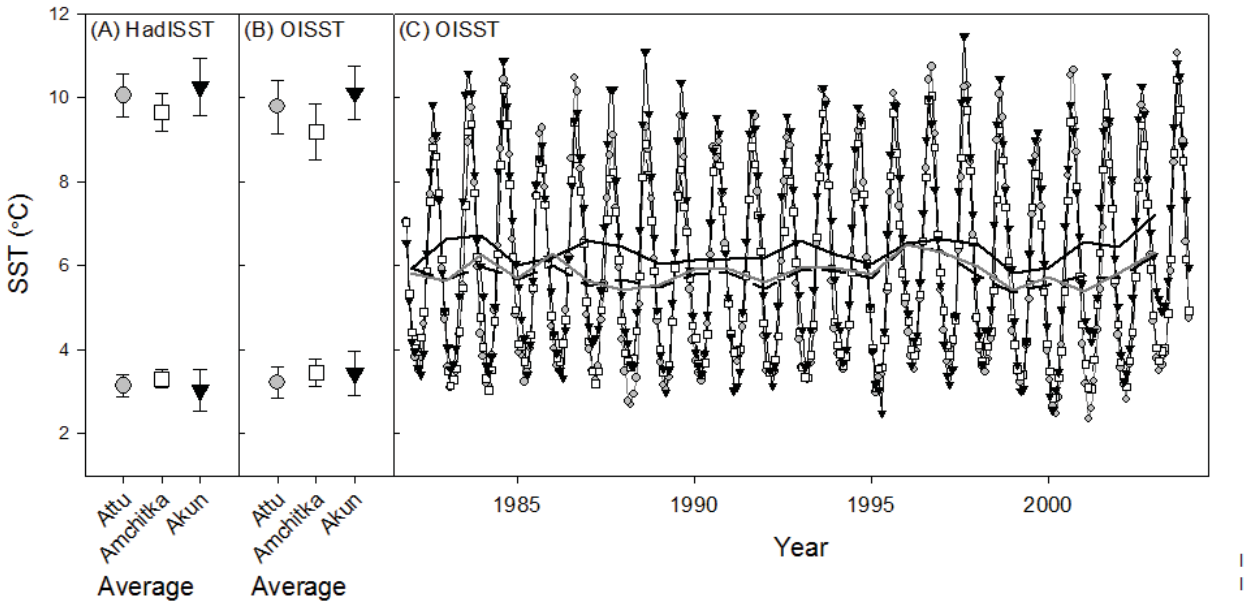

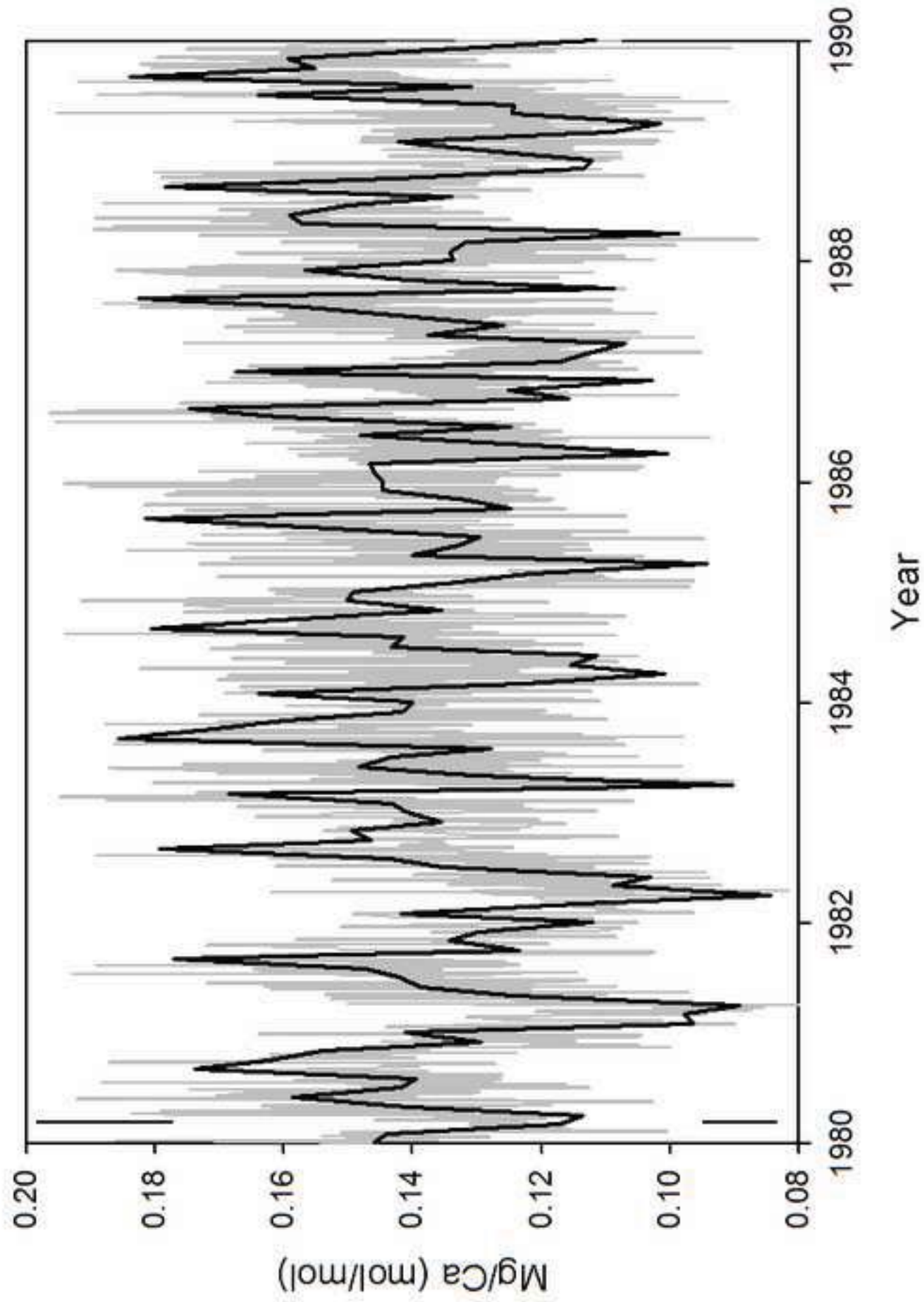

Figure 5

Figure 6

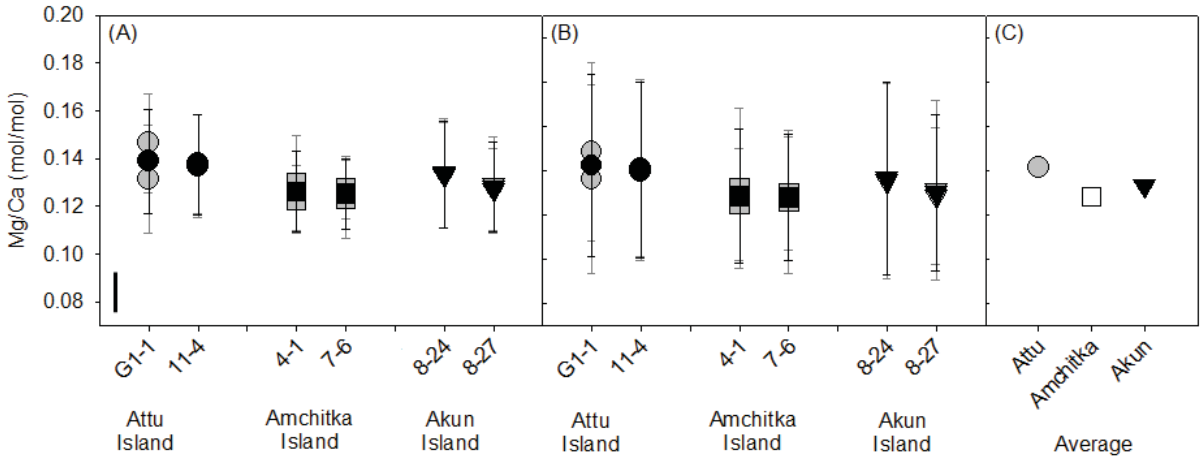

Figure 7

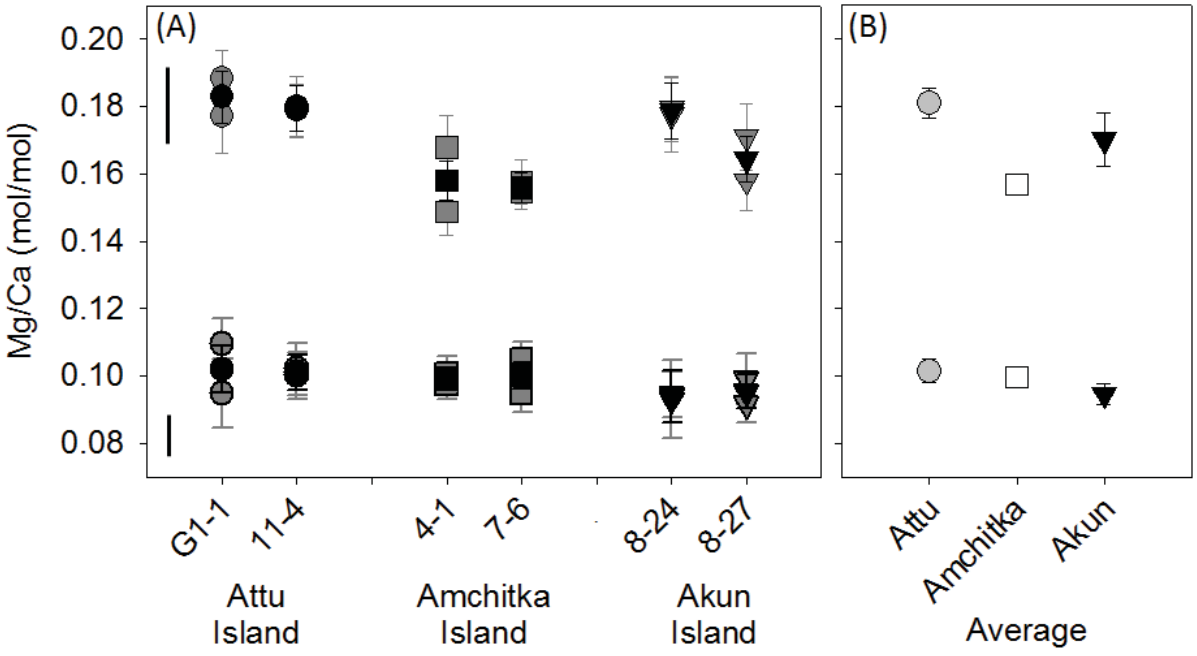

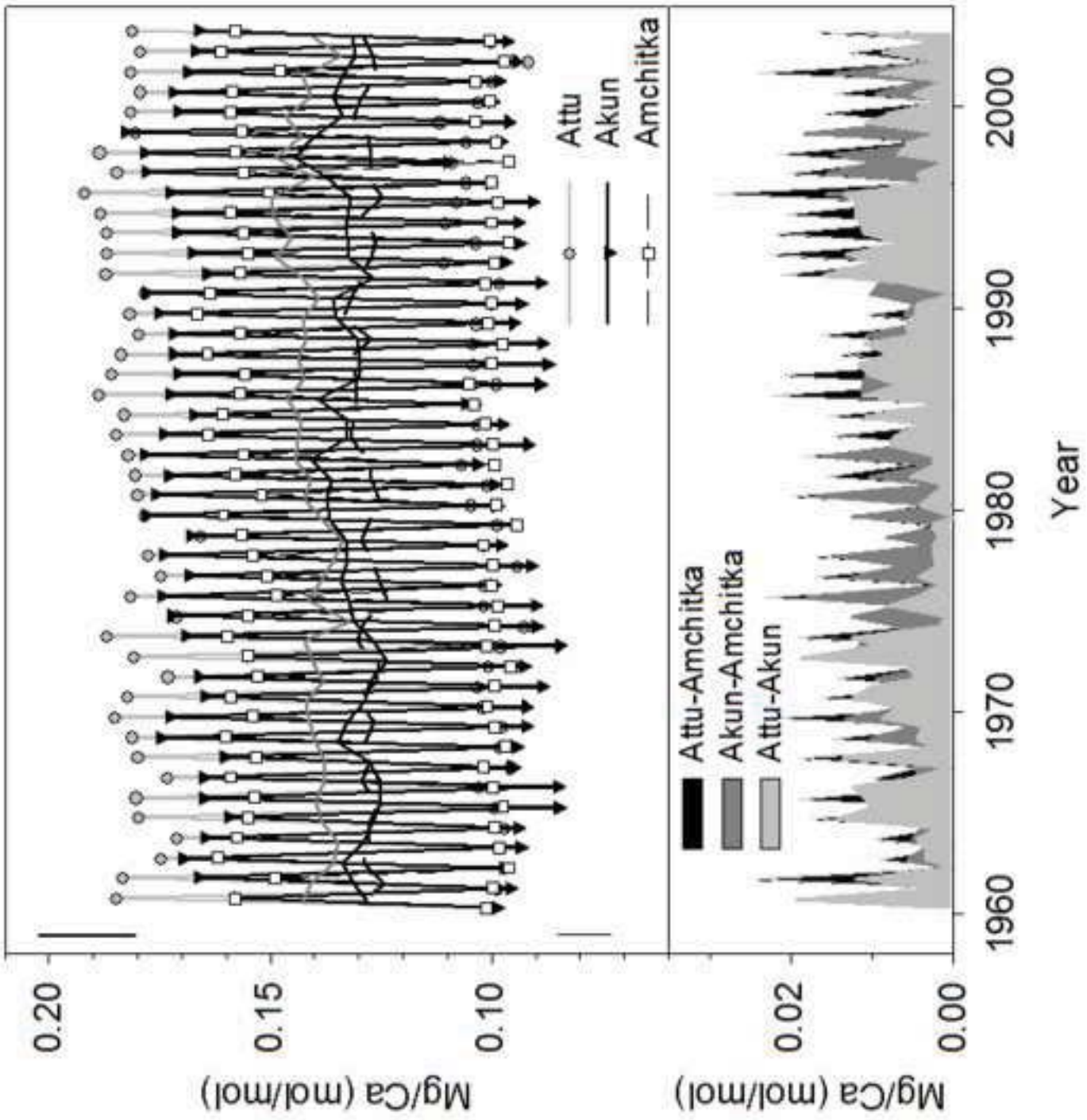
Attu
Akun
Amchitka
Attu-Amchitka
Akun-Amchitka
Attu-Akun
Mg/Ca (mol/mol)
0.20
0.15
0.10
0.02
0.00
1960
1970
1980
1990
2000
Year

Figure 8

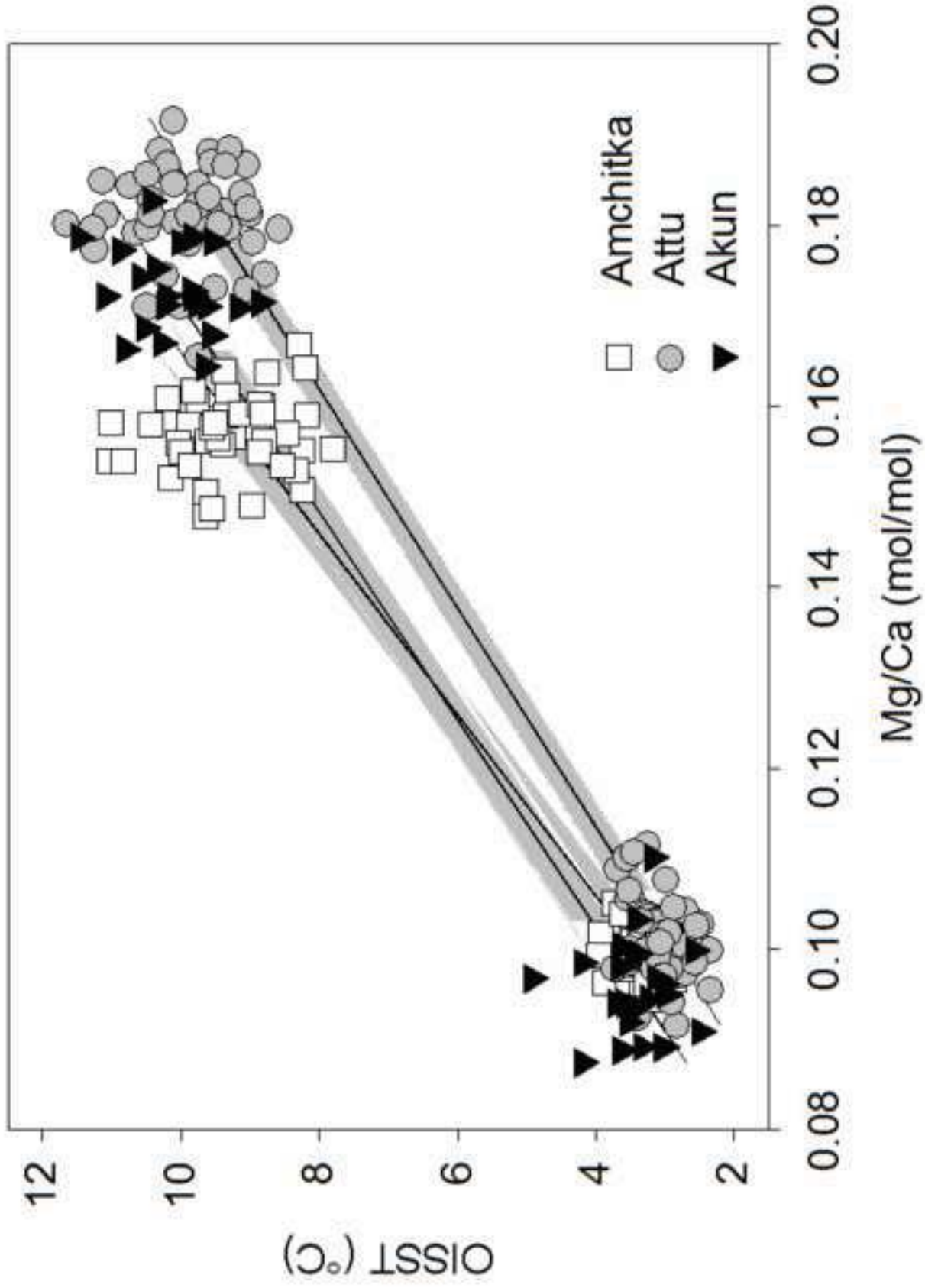
Amchitka
Attu
Akun
OISST (°C)
Mg/Ca (mol/mol)
2
4
6
8
10
12
0.08
0.10
0.12
0.14
0.16
0.18
0.20

Figure 9

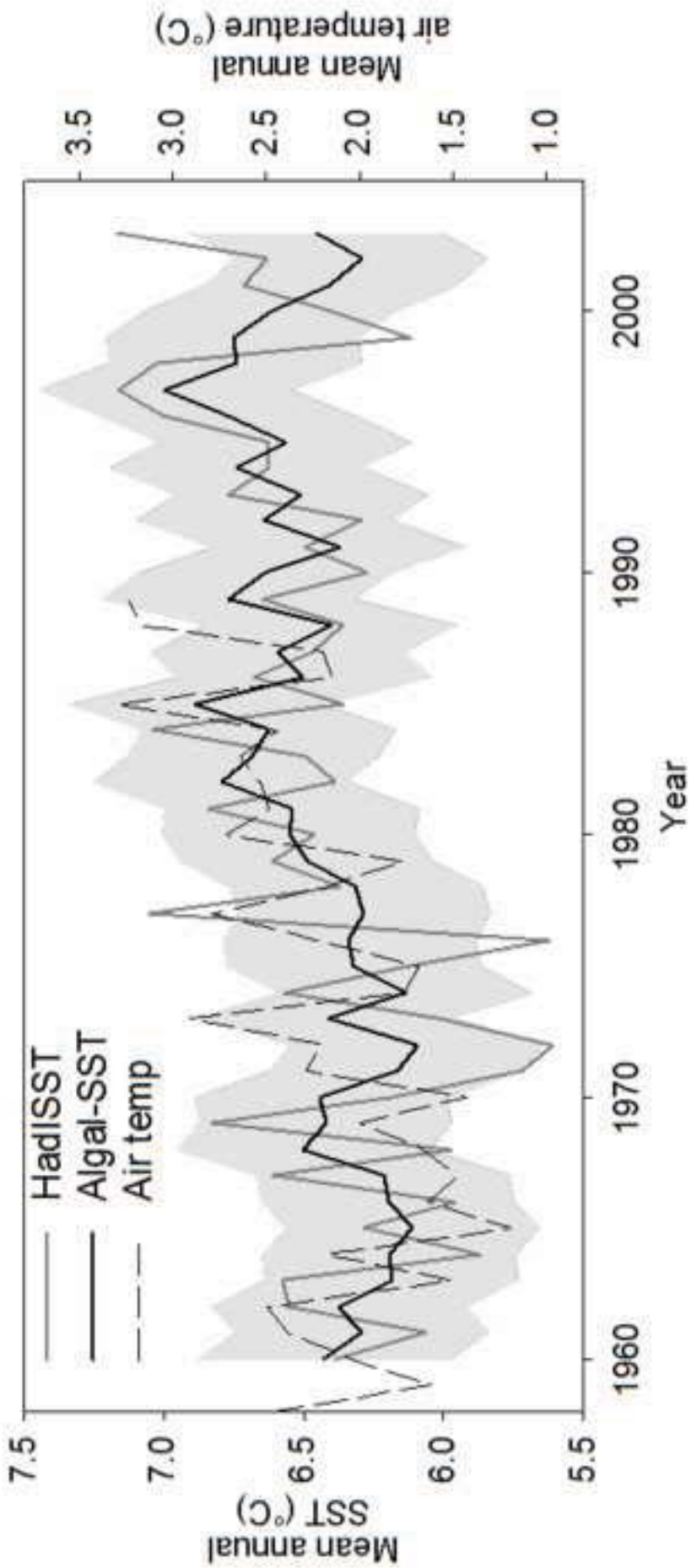

Figure 10

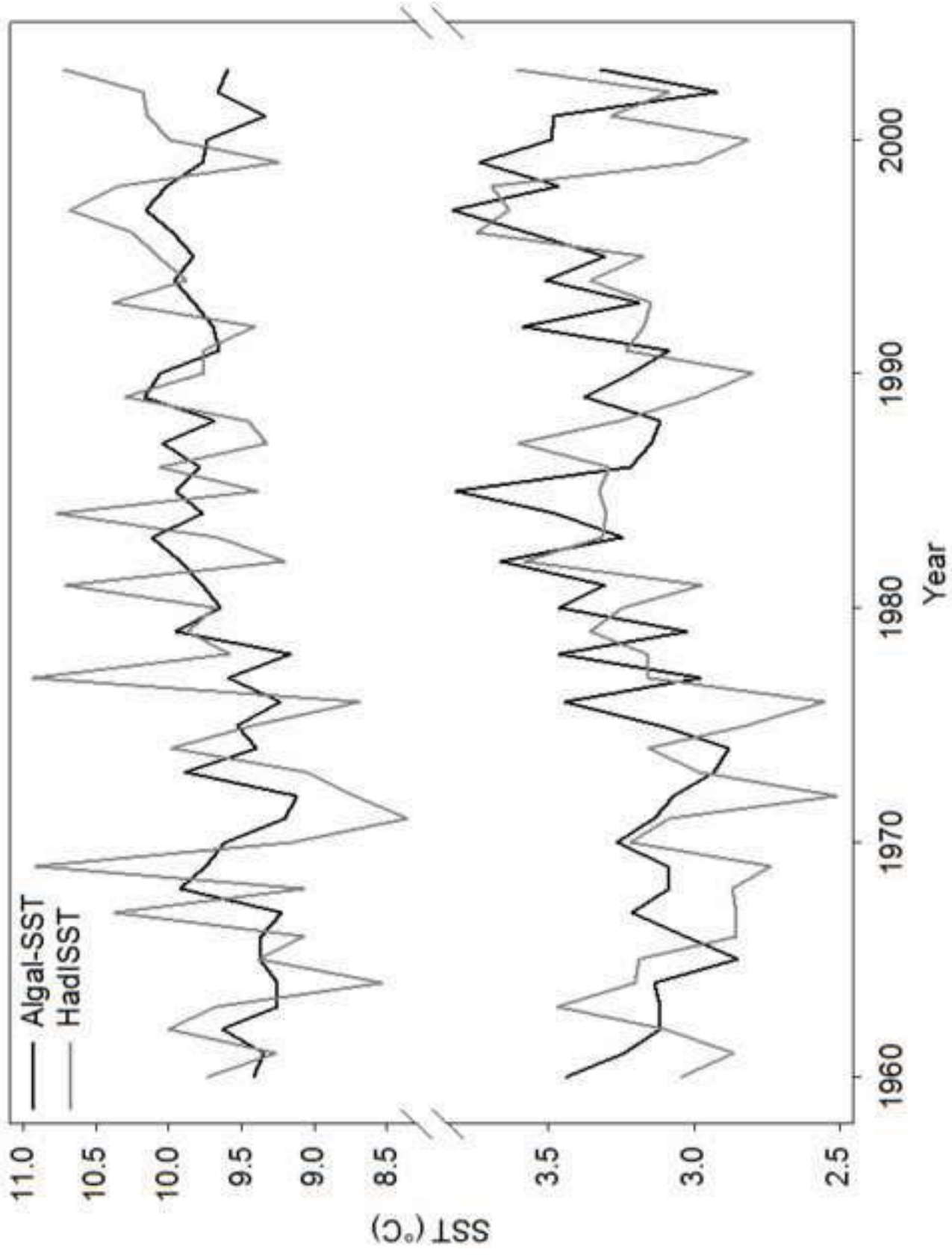

Figure 11

Figure 12